High snow accumulation on Amundsen Sea coastal ice rise, West Antarctica

Sang-Bum HONG[1] (iD), Yalalt NYAMGEREL[2] (iD),
Won Sang LEE[1] (iD) and Jeonghoon LEE[2]* (iD)

[1]*Division of Glacial Environment Research, Korea Polar Research Institute, 26, Songdomirae-ro, Yeonsu-gu, Incheon 21990, Korea*

[2]*Department of Science Education, Ewha Womans University, 52, Ewhayeodae-gil, Seodaemun-gu, Seoul 120-750, Korea*

* corresponding author <jeonghoon.d.lee@gmail.com>

Abstract: Polar snow and its accumulation preserve valuable information derived from the atmosphere on past climate and environmental changes in high resolution, particularly in coastal sites. A 2.5-m snow-pit was excavated from the coastal ice rise (Moore Dome) near Amundsen Sea region in February 2012. This study evaluated the isotopic and chemical compositions in the snow-pit and compared them with meteorological variables. Based on the seasonal peaks of the MSA and $nssSO_4^{2-}$ together with $\delta^{18}O$, δD, and d-excess, the snow-pit record was corresponded to accumulation during austral winter 2011 to summer 2011/2012. The annual mean accumulation rate was assumed thus to be as large as or even higher than 1.03 m w.e. yr^{-1} at this site. A relatively warm winter temperature in 2011 was traceable in the variations of $\delta^{18}O$, δD, and *d*-excess. This study emphasizes the importance of the high snow accumulation observed at this site in providing valuable information on sub-annual variations in climate and environmental changes through the study of longer ice cores.

Keywords: Antarctica, Bear Peninsula, Moore Dome, snow-pit.

Introduction

Snow-pits, firn cores, and ice cores provide us with excellent records of the past climate and environment from Antarctica where instrumental and meteorological data are rare and short (Jouzel *et al.* 2007; Sinclair *et al.* 2010; Klein *et al.* 2019). The chemical and isotopic components of snow-pits and ice cores give us insights to past climatic and atmospheric conditions, and changes in sources of water vapor or aerosol (Delmotte *et al.* 2000; Stenni *et al.* 2000; Sinclair *et al.* 2010; Rhodes *et al.* 2012; Tuohy *et al.* 2015). Significant environmental and climatic changes have been observed in the Antarctic regions over the past decades (Parkinson and Cavalieri 2012; Sinclair *et al.* 2014; Raphael *et al.* 2016; Swetha Chittella *et al.* 2022). The Antarctic regions are increasingly acknowledged as vital and dynamic components of the Earth's climate system due to their pivotal role in interaction with atmosphere, hydrosphere, biosphere, and cryosphere systems.

The Amundsen Sea sector of West Antarctica is a critical site in terms of the rapid ice loss, particularly for the flowing glaciers in the Amundsen Sea Embayment due to the intrusion of warm circumpolar deep water through the base of coastal ice shelves coupling with variabilities in regional atmospheric circulation (Dinniman *et al.* 2012; Mouginot *et al.* 2013). The regional atmospheric circulation is highly dependent on the strength and location of the low-pressure center over Amundsen Sea sector, *i.e.*, Amundsen Sea Low (ASL) (Fogt *et al*. 2012), which makes this region experience more variable atmospheric circulation than any other regions (Connolley 1997) in Antarctica. The change of the ASL is further influenced by the Southern Annular Mode (SAM) (Turner *et al*. 2017). Thus, there is particular interest in the linkage between surface mass balance and changes in pressure systems in the Ross-Amundsen and Bellingshausen Sea sectors. In addition, the Southern Hemisphere polar jet is strongly tied to the pattern of the SAM (Fogt *et al.* 2012). Particularly, the strengthening of westerly wind linked to the positive phase of SAM affects the mass balance of the coastal Antarctica (Zwally *et al*. 2021). Moreover, the multi-decadal changes in Antarctic surface mass balance are controlled by the combination of SAM and El Ninõ-Southern Oscillation (Kim *et al.* 2020).

A recent numerical study of the West Antarctic Ice Sheet (Feldmann and Levermann 2015) reported that a complete disintegration of the West Antarctic marine ice-sheet will be taking place on a millennial timescale, leading to raise of the global sea level by at least 3 m, if the Amundsen Sea Sector is destabilized, which is in play. The consequent widespread thinning may cause the ice divides to migrate into the drainage basins of the Filchner-Ronne and Ross ice shelves, eventually inducing destabilization of those ice shelves. Another important information characterizing the Amundsen Sea sector is snow accumulation records from ice core, revealing spatio-temporal trends in ice-sheet mass-balance

in the region (Thomas *et al.* 2017), that correlates with sea ice extension (Winstrup *et al.* 2019).

Ice coring in coastal Antarctic areas is an emerging research subject in recent years in the context of ice-ocean-atmospheric interactions (Neff 2020; Mulvaney *et al.* 2021). In particular, regions like the coasts of Amundsen and Bellingshausen seas, that are closer or central to the warming and melting locations, are recommended for additional records (Steig and Neff 2018). Ice rises and ice rumples are features that are locally elevated and grounded within or in the margins of ice shelves or ice streams (Matsuoka *et al.* 2015). In general, the snow accumulation rate is high in the coastal sites and the ice flow on the ice rises is usually slow. This unique glaciological setup facilitates the sites in better preserving records of past deglaciation, climate, and ice flow dynamics (Matsuoka *et al.* 2015). Additionally, obtaining ice cores from coastal regions is more favorable in terms of logistical challenges compared to extracting long ice cores from inland sites (Matsuoka *et al.* 2015; Vega *et al.* 2016). Although there are potential local influences on the snow accumulation in ice rises (Vega *et al.* 2016), the ice core records from the sites can serve as a tracer for past atmospheric circulation (Emanuelsson *et al.* 2018). Additionally, the analysis of water stable isotopes in ice cores from West Antarctica can provide insights into temperature and the origins of moisture (Steig *et al*. 2013).

A site-based evaluation of isotopic and chemical compositions in present-day snow is important to interpret the paleoclimate records from ice cores (Stenni *et al.* 2000; Tuohy *et al.* 2015; Stenni *et al.* 2017). Thus, there is a need to improve site-based records in Antarctica due to the significant spatial and temporal variabilities in snow accumulation and air temperature (Masson-Delmotte *et al.* 2008; Yang *et al.* 2018) and the sparse instrumental data (Stenni *et al.* 2000; Tuohy *et al.* 2015). This study aims to characterize the isotopic and ionic compositions of snow deposited in seashore near the Amundsen Sea sector. High snow accumulation in the coastal site reveals more high-resolution information in the chemical and isotopic compositions in the snow-pit. Thus, this study can serve as a background investigation for future studies on longer ice cores.

Materials and methods

Study area and sampling. — A 2.5-m deep snow-pit was excavated from the top of the Moore Dome (74°21′45.6″S, 111°20′54.0″W) in Bear Peninsula, West Antarctica on February 17–19, 2012, during the Amundsen Sea expedition by Korea Polar Research Institute (KOPRI) (Fig. 1). Bear Peninsula is in the central location of the Amundsen Sea Embayment and adjacent to the Dotson ice shelf and the north-west side of the Thwaites Glacier (Johnson *et al.* 2017). Particularly, the Thwaites Glacier is of special interest because it is the second
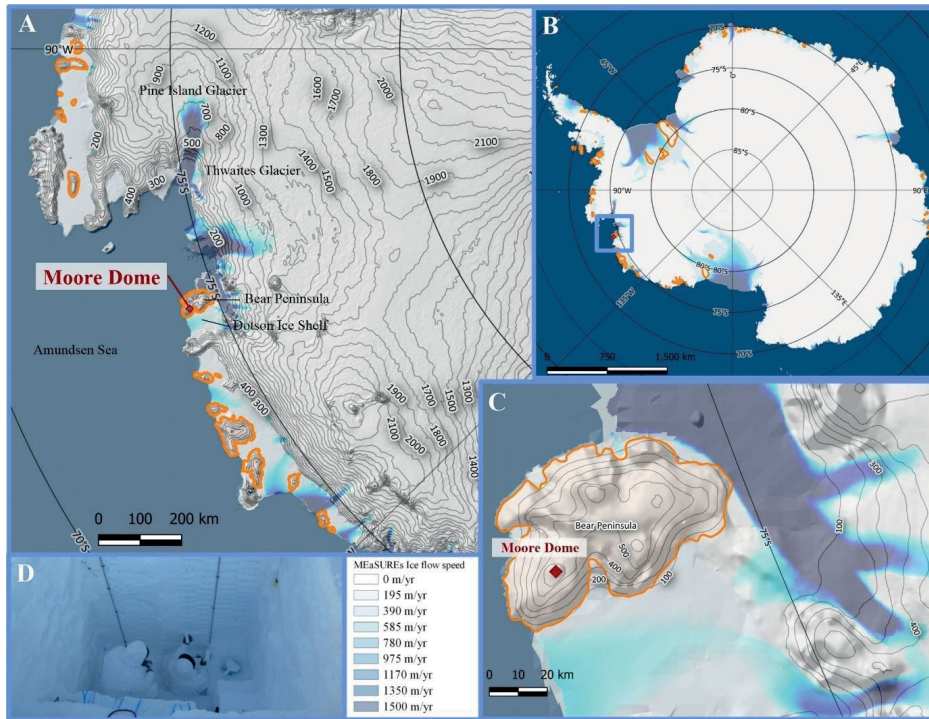
Fig. 1. Location of the snow-pit (red rhombus symbol) at Moore Dome ice rise in Bear Peninsula, West Antarctica is shown (**A**, **B**, **C**). Ice rises contoured in orange and maps are generated by the Quantarctica GIS package (Matsuoka *et al.* 2015, 2021). Ice flow speed map (MEaSUREs InSAR-based Antarctica Ice Velocity Map, version 2, 450 m resolution) (Rignot *et al.* 2011, 2017; Mougnot *et al.* 2012, 2017), RAMP2 virtual elevation model (200 m) (Liu *et al.* 2015) with CryoSat-2 elevation contours (100 m) (Helm *et al.* 2014) are shown. The snow-pit sampling procedure is shown (**D**).

largest marine ice stream in West Antarctica (Sutterley *et al.* 2014). Specifically, the Thwaites grounding zone retreated at a rate of >2.1 km yr^{-1} and is further projected to retreat rapidly (Graham *et al.* 2022). Moreover, continuous ice loss has been observed in the Crosson and Dotson ice shelves since the 1990s (Lilien *et al.* 2018). The sub-ice sediments also showed the fingerprints of the ice stream of the Thwaites and the Pine Island Glaciers (Pereira *et al.* 2020). Generally, the snow accumulation rate is high in the coastal sites and the ice flow on the ice rises is usually slow (Scarchilli *et al.* 2011; Matsuoka *et al.* 2015). Ice rise records will provide high resolution information on atmospheric and oceanic conditions in coastal areas (Matsuoka *et al.* 2015; Vega *et al.* 2016), and thus would provide a good background for long-term climate variability based on modern observations.

The site is a dome-shaped ice rise *ca.* 20 km from the seashore of the Amundsen Sea embayment. The ice thickness was estimated to be >300 m based on the GPR survey (Mala ProEX system with RTA 50 MHz antenna) with an ice

velocity of 0.16 m s^{-1}. Annual mean air temperature is –12.7°C, ranging between –44.0°C and 4.8°C, based on the temperature record from Bear Peninsula automatic weather station (AWS) from 2011 to 2021 (Antarctic Meteorological Research and Data Center 2021). The prevailing winds are directed from the east (22.5% of total counts), north (21.4% of total counts), and southeast (18.4% of total counts), based on the AWS observations during the period from 2011 to 2017. Moreover, the mean wind speed was recorded to be <10 m s^{-1} (73.8% of total counts) based on the observations during the period from 2011–2016 (Antarctic Meteorological Research and Data Center 2021).

Snow-pit was sampled *ca.* 200 m away from the Moore Dome camp to minimize the influence of human activities during field activity period. The wall of the snow-pit was removed using precleaned low-density polyethylene (LDPE) shovels. A total of 50 samples was obtained with 5 cm resolution. During the field work, snow densities and temperatures were measured every 5 cm and 10 cm, respectively (Fig. 2). Samples were collected into precleaned
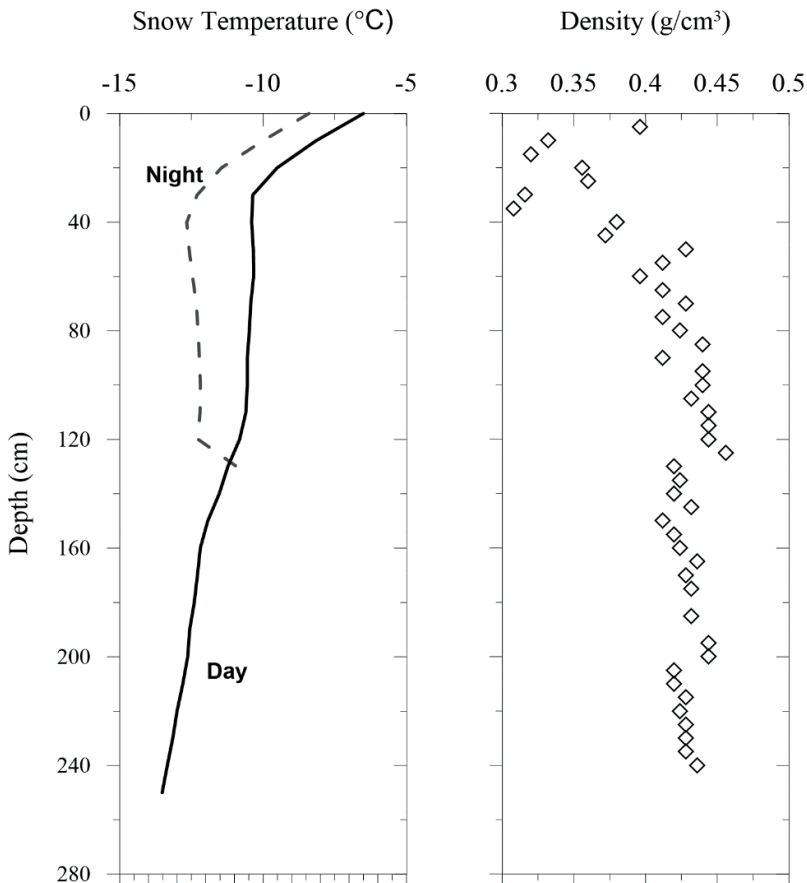
Fig. 2. Vertical profiles of snow temperature and density in the Moore Dome snow-pit.

polyethylene containers and transported to KOPRI in South Korea. The sampling procedure was designed to prevent sample contamination followed the procedure of Kwak *et al*. (2015). The snow samples were stored below –20°C until melting prior to chemical analysis.

Analytical methods and data analysis. — The snow samples were melted at room temperature and analyzed for water isotopes ($\delta^{18}O$ and δD) by a cavity ring-down laser-spectroscopy (L1102-i, L2130-i; Picarro Inc., USA) at KOPRI. The δD and $\delta^{18}O$ express the relative ratios of D/H and $^{18}O/^{16}O$ in the sample to those in the Vienna Standard Mean Ocean Water (VSMOW), respectively. The standard materials including VSMOW, Greenland Ice Sheet Precipitation, and Standard Light Antarctic Precipitation from the International Atomic Energy Agency were used for calibration. Moreover, an in-house reference prepared from Antarctic snowmelt (-34.69‰ for $\delta^{18}O$ and -272.30‰ for δD) was measured every 10 samples to monitor the operation of the analyzer (Kim *et al.* 2022). The analytical reproducibility was < 0.1‰ and < 1‰ for $\delta^{18}O$ and δD, respectively. The deuterium excess (*d*-excess, $\delta D = 8 \times \delta^{18}O - 10$), which represents the deviation from the global meteoric water line (GMWL), was also estimated (Craig 1961). Ions (Na^+, K^+, Ca^{2+}, Mg^{2+}, NH_4^+, Cl^-, SO_4^{2-}, NO_3^- and $CH_3SO_3^-$ or MSA) were analyzed using a two-channel ion chromatography system combined with two Dionex ion chromatography sets (Thermo Fisher Scientific Inc., USA) at KOPRI. Anions were analyzed using a Dionex model ICS-2000 with an IonPac AS15 column and KOH eluent (6–55 mM), and cations were measured using a Dionex model ICS-2100 with an IonPac CS12A column and MSA eluent (20 mM). The analytical detection limit, reproducibility, and accuracy were, 0.01–0.26 µg L^{-1}, 0.4–17.4%, and 4.5–12.0% for cations and 0.02–0.26 µg L^{-1}, 0.1–27.6%, and 1.3–5.6% for anions (Hong *et al.* 2012), respectively. Using the theoretical ratio of a specific ion to Na^+ in sea water (Pilson 2013), the non-sea-salt (nss) fraction of the ions was estimated to separate the contribution of sea-spray using the equation assuming that Na^+ was exclusively of sea-salt origin (Kuramoto *et al.* 2011):

$$[nssX] = [X] - (X/Na^+)_{sw} \cdot Na^+$$

where X is the target ion and $(X/Na^+)_{sw}$ is the ratio of that ion and Na^+ in seawater.

Meteorological data from the AWS located around 25 km east of the snow-pit site in Bear Peninsula (Antarctic Meteorological Research and Data Center 2021) was compared with the snow-pit data. Moreover, sea ice extent (SIE) data in the Bellinghausen-Amundsen Sea sector was retrieved and compared to the snow-pit data (Parkinson and Cavalieri 2012). The location map and distribution of ice rises in the map were generated by the Quantarctica GIS package (Matsuoka *et al*. 2015, 2021).

Results and interpretation

Isotopic compositions of the snow-pit. — The $\delta^{18}O$-δD diagram is shown in Fig. 3. Processes other than evaporation, such as an isotopic exchange between liquid water and ice or between water vapor and ice can modify the slope of the $\delta^{18}O$ *vs.* δD (Earman *et al.* 2006; Lee *et al.* 2010). Evaporation, sublimation, and percolation of summertime meltwater are considered major processes influencing the isotopic feature of original snow layers (Ham *et al.* 2019). In this study, the slope of the linear relationship for the snow-pit is 7.7, similar to the slope of 8 of the global meteoric water line (GMWL) (Craig 1961). The small difference in slope between GMWL and the snow-pit may be insignificant, but the slight difference may indicate isotopic modification of the sublimation of snow (Earman *et al.* 2006; Lee *et al.* 2010). The deviation of the GMWL in intercept

$$\delta D=(7.7\pm0.15)*\delta^{18}O+(1.1\pm2.15)$$
$$R^2=0.98$$
$$n=50$$
$$p<0.001$$
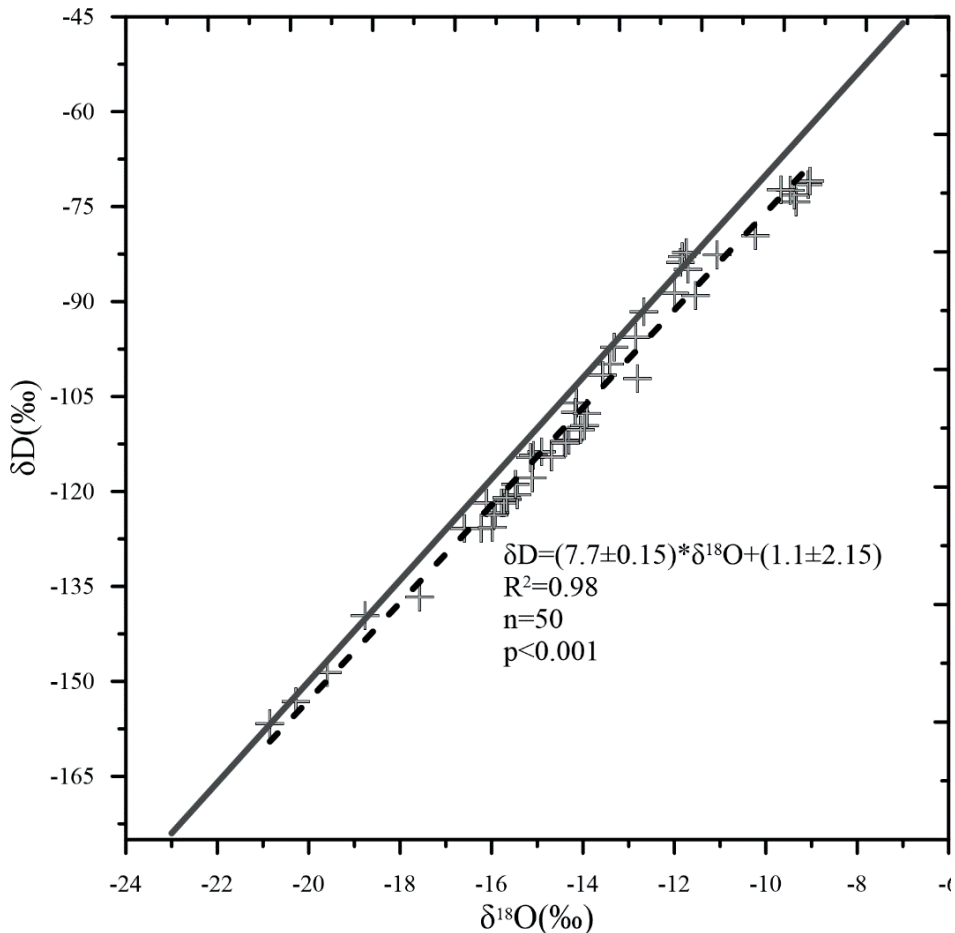
Fig. 3. $\delta^{18}O$-δD diagram of the snow-pit marked as the dashed line with the Global Meteoric Water Line of Craig (1961) marked as the solid line.

can also occur from humidity differences of the water vapor source. The smaller intercept may reflect smaller kinetic effects during evaporation over the nearby ocean than for the worldwide average (Jouzel and Merlivat 1984).

Figure 4 shows the vertical profiles of $\delta^{18}O$, δD, and deuterium-excess (d-excess; $d=\delta D–8\ \delta^{18}O$) obtained from the snow-pit. The $d^{18}O$ values ranged between –20.85‰ and –9.03‰ while the δD values fluctuated from –156.65‰ to –70.96‰ (Table 1). The mean $\delta^{18}O$ and δD values (–14.05‰ and –107.11‰, respectively) are in a similar range to records in seashore sites (Delmotte *et al.* 2000; Hur *et al.* 2022) and relatively enriched values compared to other distant sites (Masson-Delmotte *et al.* 2008; Nyamgerel *et al.* 2020). This indicates the site proximity to the ocean. In general, the sinusoidal trends in $\delta^{18}O$ and δD of polar snow-pit and ice cores primarily represent their conventional correlation to the annual temperature cycle (Dansgaard 1964; Petit *et al.* 1999; Kuramoto *et al.* 2011; Küttel *et al.* 2012). The $\delta^{18}O$ and δD of the snow-pit show no clear increasing trend, which may clearly represent the summer peak. Rather, by comparing the gradual increase in the MSA and $nssSO_4^{2-}$, the single summer layer can be detected, which leads us to conclude that the snow accumulation does not exceed the annual scale.

Chemical compositions of the snow-pit. — The variations of ions are presented in Fig. 4 and Pearson's correlation matrix is shown in Table 2. Sea salt ions (Na^+, K^+, Mg^{2+}, Ca^{2+}, Cl^-, and SO_4^{2-}) positively correlated with each other (r > 0.76, p < 0.01). A high concentration of sea salts commonly occurs in the winter layer due to intensive storms which transport fragile sea-salt crystals formed above the sea ice surface (Udisti *et al.* 1998; Rankin *et al.* 2000; Abram *et al.* 2007). The sea salt ions in the snow-pit show no clear seasonal increase; rather, they show a less-varied distribution. Moreover, the Cl^-/Na^+ ratio was similar, except for the peak at 1.7–1.8 m, and less varied to those in seawater (1.18), indicating the dominant and consistent supply from sea salt aerosols. The excess Cl^- peak at 1.7–1.8 m may represent the winter snow layer related to sea ice extent (Pasteris *et al.* 2014). For the average, non-sea-salt portion of Mg^{2+} and Ca^{2+} were 51.1% and 34.8%, respectively. This indicates their potential emission from continental mineral dust (Nyamgerel *et al.* 2020). An enhancement of $nssCa^{2+}$ in spring was observed in the other studies relating to wind-induced transport of crustal dust due to cyclonic activity (Rhodes *et al.* 2012).

NO_3^- shows a moderate positive correlation (r > 0.45) with d-excess and NH_4^+ with two distinct peaks at 1.15 and 1.85 m depth. In addition, at the bottom depth, there was an increasing trend. Due to the shortness of the period covered in the snow-pit data, it is difficult to accurately interpret these values. Moreover, it is necessary to consider random variabilities induced by various precipitation timing and wind effect (Pasteris *et al.* 2014). NH_4^+ shows an increase in summertime with biogenic sulfur (Legrand and Mayewski 1997). An enhancement of NO_3^- is usually observed during spring and summer periods, relating to more efficient stratosphere/troposphere exchange and higher irradiance (Caiazzo
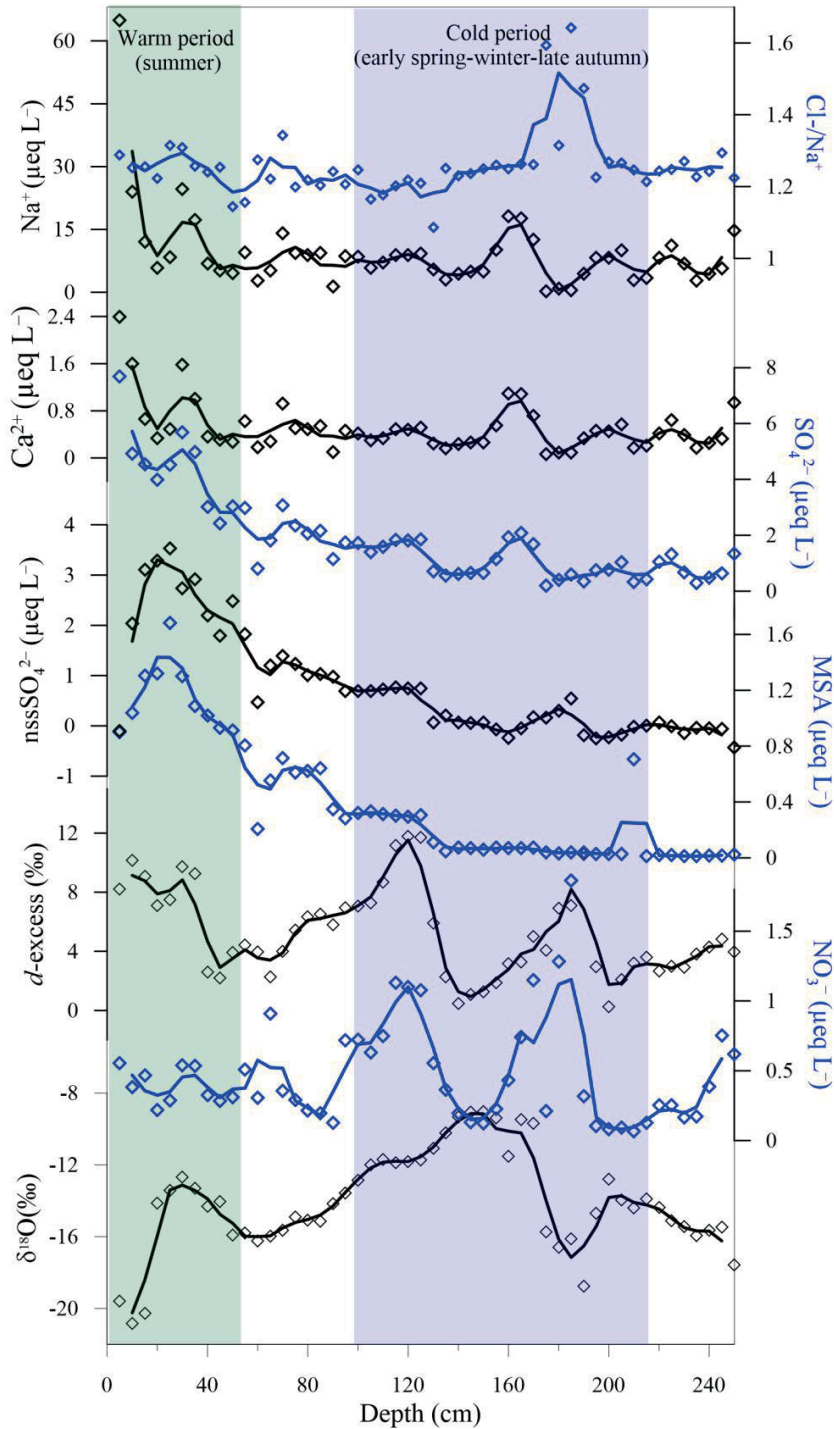
Fig. 4. Depth *vs.* $\delta^{18}O$, *d*-excess, NO_3^-, MSA, $nssSO_4^{2-}$, SO_4^{2-}, Ca^{2+}, Na^+, and Cl^-/Na^+. Thick lines represent the three-point running average profiles.

Table 1.

Mean, standard deviation, minimum, maximum values of isotopic ratios (‰) and ion concentrations (µeq L^{-1}).

Variables	Mean	Standard deviation	Standard error	Minimum	Maximum	Median
δD	−107.11	21.97	3.11	−156.65	−70.96	−111.06
δ^{18}O	−14.05	2.83	0.40	−20.85	−9.03	−14.24
d-excess	5.27	3.05	0.43	0.25	11.76	4.34
Na$^+$	9.31	9.65	1.37	0.27	64.95	8.24
NH$_4^+$	0.25	0.13	0.02	0.06	0.57	0.22
K$^+$	0.21	0.25	0.04	0.00	1.57	0.16
Mg^{2+}	2.20	2.15	0.30	0.26	14.00	1.85
Ca^{2+}	0.52	0.43	0.06	0.07	2.40	0.41
MSA	0.40	0.45	0.06	0.01	1.68	0.25
Cl$^-$	11.67	12.44	1.76	0.43	83.69	10.18
SO$_4^{2-}$	1.88	1.61	0.23	0.19	7.69	1.49
nssSO$_4^{2-}$	0.76	1.05	0.15	−0.43	3.53	0.38
NO$_3^-$	0.47	0.37	0.05	0.07	1.86	0.34

Table 2.

Correlation matrix for the isotopic ratios and ion concentrations in the snow-pit. Correlation coefficient values > 0.4 at p value < 0.01 are shown in bold.

	δD	δ^{18}O	d-excess	NO$_3^-$	Cl$^-$	SO$_4^{2-}$	MSA	Na$^+$	NH$_4^+$	K$^+$	Mg^{2+}	Ca^{2+}
δD	1.00											
δ^{18}O	**0.99**	1.00										
d-excess	−0.15	−0.28	1.00									
NO$_3^-$	0.09	0.02	**0.51**	1.00								
Cl$^-$	−0.22	−0.25	0.26	0.04	1.00							
SO$_4^{2-}$	−0.26	−0.31	**0.45**	0.04	**0.76**	1.00						
MSA	−0.26	−0.30	0.38	−0.10	0.32	0.83	1.00					
Na$^+$	−0.21	−0.24	0.27	0.05	**1.00**	**0.76**	0.32	1.00				
NH$_4^+$	0.18	0.12	0.45	**0.50**	0.35	**0.56**	0.42	0.36	1.00			
K$^+$	−0.19	−0.22	0.27	0.08	**0.99**	**0.74**	0.30	**0.99**	0.39	1.00		
Mg^{2+}	−0.23	−0.26	0.28	0.05	**1.00**	**0.77**	0.34	**1.00**	0.37	**0.99**	1.00	

et al. 2017). Moreover, secondary peaks of NO_3^- were also observed in the late winter in ice cores from the West Antarctic Ice Sheet (Pasteris *et al.* 2014).

MSA and $nssSO_4^{2-}$ are mainly sourced from marine biogenic activity during the austral spring and summer period (Udisti *et al.* 1998) and the emission is large, especially in coastal sites (Dixon *et al.* 2004; Jonsell *et al.* 2005; Rhodes *et al.* 2012) Moreover, it can be derived from crustal erosion and volcanic emissions (Delmas *et al.* 1992; Legrand and Mayewski 1997). In this snow-pit, the MSA and $nssSO_4^{2-}$ were high in top layers, with a gradually decreasing trend starting from 0.2 to 1.3 m depth. These increased values correspond to the summer period relating to a strong seasonality of dimethyl sulfide production (Udisti *et al.* 1998). Kofftman *et al.* (2017) reported the rapid transport and detection of sulfate sourced by the Puyehue-Cordón Caulle volcanic eruption (June 2011) in West Antarctic site during the winter of 2011. In the Moore Dome snow-pit, the $nssSO_4^{2-}$ shows no clear signal to this volcanic eruption which may be due to the spatial heterogeneity of this volcanic deposition or the shortness of the snow-pit record.

Snow dating and accumulation. — A density measurement showed a slight increase from 356.0 kg m^{-3} to 436.0 kg m^{-3} with increasing depth. Moreover, the snow temperatures were below –6.5°C both at daytime and nighttime. In the daytime, the snow temperature ranged between –6.5 to –13.5°C with a decreasing trend as depth increased (Fig. 2). No melted layers or ice lenses were observed in the snow-pit, which is likely to indicate good preservation of snow layers at this snow depth. However, the snow accumulation on ice rises can be affected by the occurrence of ice lenses (Vega *et al.* 2016) and the precipitation amount, and post-depositional effects must be considered in the interpretation of ice rises records.

We assume that the top layers (0–0.5 m) correspond to mid to late summer based on the clear increasing trend with MSA and $nssSO_4^{2-}$. $NssSO_4^{2-}$ were used as summer indicators in other coastal cores (Thomas *et al.* 2015). Moreover, the depth range 1.5–2.5 m is characterized by very low concentrations of MSA and $nssSO_4^{2-}$, which indicate austral winter period. Thus, the Moore Dome snow-pit is likely to cover austral summer 2011/2012 to winter 2011. The snow depth of 2.5 m was estimated to correspond to 1.03 m in water depth by using the mean density of the snow-pit (412.7 kg m^{-3}). Austral summer 2011/2012 peaks are certain; however, it is not possible to detect autumn 2011 or the previous summer (2011/2010) due to the shortness of the snow-pit record. At this point, although the Moore Dome snow-pit is short (not full year), we carefully state that the snow accumulation is relatively high at this period and comparable to other estimates in the coastal ice rises on Fimbul Ice Shelf (0.24, 0.68, 0.70 m w.e. yr^{-1}) (Vega *et al.* 2016) and in coastal areas in Thwaites Glacier (0.67 m w.e. yr^{-1}) (Medley *et al.* 2013). The precipitation data by the ERA-Interim reanalysis dataset in the nearest (20–70 km to the study site) two grid points (74.24°S, 111.75°W; 75°S, 111°W) (Dee *et al.* 2011) between 2011 to 2012 were very low (0.015 m w.e. yr^{-1})

compared to the snow accumulation in the snow-pit, which simply may be a shift due to single point comparison. The annual average snow accumulation at the Bryan Coast ice cores (*ca.* 190 km to the coast) was constantly around 0.40 m w. e. yr^{-1} before the 1900s, however increased with a rate of 0.0015 m w.e. yr^{-1} in the recent decade (2000–2009). This increasing trend in snow accumulation rate was large, particularly in the recent decade (2000–2009), related to the ASL deepening (Thomas *et al.* 2015). Moreover, a historical (up to 200 years) snow accumulation in the ice cores from Pine Island-Thwaites drainage systems was 0.38 m w.e. yr^{-1} on average (Kaspari *et al.* 2004).

The seasonality of δ^{18}O can be assumed, with a summer high of –12.67‰ at 0.3 m and a winter low of –18.77‰ at 1.9 m. This variation may be reasonable to assume as summer and winter peaks. Thus, we can assume that the δ^{18}O at 0.3 m was the summer (Dec to Jan) peak in 2012 with MSA and nssSO$_4^{2-}$. Comparable ranges can be seen in the monthly mean air temperature in austral summer (–6.4 ±1.0°C) and winter periods (–18.1±3.1°C) during the years between 2011 and 2021.

At the middle depth of the snow-pit, δ^{18}O showed enriched values and reached –9.07‰ (1.45 m), which is higher than the expected summer peak (–12.67‰) at 0.3 m. Moreover, *d*-excess and NO$_3^-$ showed significant peaks at this depth range (1.1–1.2 m and 1.75–1.85 m) (Fig. 4). It likely indicated a particular event-based variation during this period. Moreover, it can be related to the temperature range (summer and winter months) which was slightly lower in 2011 (–8.0°C and –14.2°C) compared to 2012 (–6.8°C and –21.0°C). Particularly, mean temperatures in July and August 2011 were recorded higher than those in April, May, and June. A relatively higher and largely varied temperature in 2011 (Fig. 5) is likely to correspond to the lower sea ice extent in winter 2011 compared to those in 2012. Further the existence of polynya during winter months could also contribute the enriched δ^{18}O observed at the middle depth (Stammerjohn *et al*. 2015). The relatively large variation was also reflected in the wind speed data during the 2011 winter. It may be assumed that the enriched δ^{18}O and δD and the significant peaks of *d*-excess and NO$_3^-$ are likely related to the meteorological conditions in the austral winter to spring in 2011. In addition, Wang *et al.* (2019) reported that the negative anomalies of cloud fraction in July 2011 (winter) induced the decrease in sea ice extent that year and was further linked to the increase in 2012.

The annual mean accumulation rate thus can be large as or even higher than 1.03 m w.e. yr^{-1}, corresponding to 2.5 m snow depth at the Moore Dome site. This high snow accumulation could be supportive to study correlations with climate variabilities (Emanuelsson *et al.* 2018). Vega *et al.* (2016) reported the three ice core records on the ice rise near western Dronning Maud Land and the water isotopes and estimated snow accumulation in these cores were preserving the linkage with atmospheric circulation patterns. Swetha Chittella *et al.* (2022) reported extreme precipitation events over the Amundsen Sea embayment, which
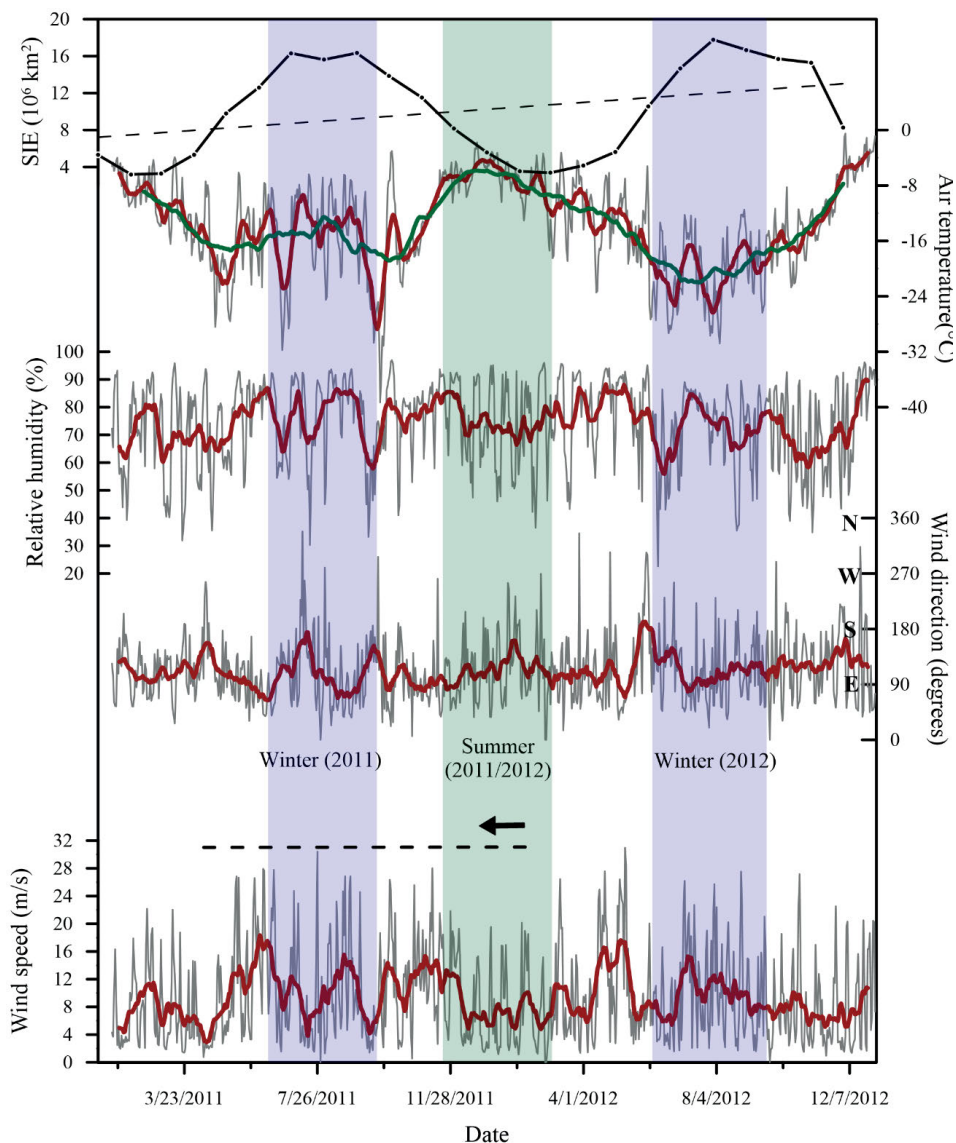
Fig. 5. Daily mean (grey line) and 15-point running averaged (red line) meteorological data between January 2011 to December 2012 in Bear Peninsula automatic weather station with monthly mean sea ice extent data. The green line is 60 day-average air temperature. Purple and green shading indicate winter and summer seasons, respectively. The horizontal dashed line and arrow indicate the period covered in the Moore Dome snow-pit. We note that the top layers of the snow-pit corresponding to the summer 2011/2012 was relatively clear, however bottom depth is roughly assumed to extend to winter 2011.

accounted for *ca.* 30% of total precipitation. It is reasonable to note that other factors would account for the snow accumulation and its temporal variation in this sector, which will be clearer with longer ice core records. For instance,

Amundsen Sea Low (ASL) pressure and its location are becoming crucial for Antarctic climate variabilities (Hosking *et al.* 2013; Sinclair *et al.* 2014). Strong winds enhanced by the ASL changes increase the sea ice cover (Raphael *et al.* 2016; Turner *et al.* 2022). Moreover, the ASL is linked to the rapid ice losses from some West Antarctic glaciers due to changes in ocean circulation (Thoma *et al.* 2008). It can be stated that high-resolution paleoclimatic records need to be studied to achieve a better understanding of the atmospheric and oceanic conditions in coastal Antarctic regions, which are the critical location for the projections on sea level rise (Jacob *et al.* 2012; Neff 2020)

Conclusion

This work analyzed the isotopic and chemical compositions of the snow deposited on the Moore Dome ice rises on the seashore of the Amundsen Sea. The seasonal increase of the MSA, $nssSO_4^{2-}$ was clearly shown and used as seasonal marker for snow dating. Based on the seasonal characteristics of these records, the 2.5 m depth of snow-pit corresponds to the deposition between the austral winter 2011 and austral summer 2011/2012. The annual mean accumulation rate was assumed thus to be as large as or even higher than 1.03 m w.e. yr^{-1} at this site. The significant variations in the $\delta^{18}O$, δD, and *d*-excess were likely to be preserving the changes in meteorological conditions in winter 2011. This led us to make a statement that the snow accumulation is high enough to preserve the sub-annual variations in climate and environmental changes in longer ice cores in this location.

References

Abram N.J., Mulvaney R., Wolff E.W. and Mudelsee M. 2007. Ice core records as sea ice proxies: an evaluation from the Weddell Sea region of Antarctica. *Journal of Geophysical Research-Atmospheres* 112: D15101. doi: 10.1029/2006JD008139

Antarctic Meteorological Research and Data Center. 2021. Bear Peninsula Automatic Weather Station, 2021 quality-controlled observational data. AMRDC Data Repository, accessed 04-11-2022. doi: 10.48567/r833-t188

Caiazzo L., Baccolo G., Barbante C., Becagli S., Bertò M., Ciardini V., Crotti V., Delmonte B., Dreossi G., Frezzotti M., Gabrieli J., Giardi F., Han Y., Hong S.B., Hur S.D., Hwang H., Kang J.H., Narcisi B., Proposito M., Scarchilli C., Selmo E., Severi M., Spolaor A., Stenni B., Traversi R. and Udisti R. 2017. Prominent features in isotopic, chemical and dust stratigraphies from coastal East Antarctic ice sheet (Eastern Wilkes Land). *Chemosphere* 176: 273–287. doi: 10.1016/j.chemosphere.2017.02.115

Connolley W.M. 1997. Variability in annual mean circulation in southern high latitudes. *Climate Dynamics* 13: 745–756. doi: 10.1007/s003820050195

Craig H. 1961. Isotopic variations in meteoric waters. *Science* 133: 1702–1703. doi: 10.1126/science.133.3465.170

Dansgaard W. 1964. Stable isotopes in precipitation. *Tellus* 16: 436–468. doi: 10.3402/tellusa.v16i4.8993

Dee D.P., Uppala S.M., Simmons A.J., Berrisford P., Poli, P., Kobayashi S., Andrae U., Balmaseda M.A., Balsamo G., Bauer P., Bechtold P., Beljaars A.C.M., van de Berg L., Bidlot J., Bormann N., Delsol C., Dragani R., Fuentes M., Geer A.J., Haimberger L., Healy S.B., Hersbach H., Hólm E.V., Isaksen L., Kållberg P., Köhler M., Matricardi M., McNally A.P., Monge-Sanz B.M., Morcrette J-J., Park, B-K., Peubey C., de Rosnay P., Tavolato C., Thépaut J-N. and Vitart F. 2011. The ERA-Interim reanalysis: configuration and performance of the data assimilation system. *Quarterly Journal of the Royal Meteorological Society* 137: 553–597. doi: 10.1002/qj.828

Delmas, R.J., Kirchner S., Palais J.M. and Petit J.R. 1992. 1000 years of explosive volcanism recorded at the South Pole. *Tellus* 44B: 335–350. doi: 10.3402/tellusb.v44i4.15461

Delmotte M., Masson V., Jouzel J. and Morgan V.I. 2000. A seasonal deuterium excess signal at Law Dome, coastal eastern Antarctica: A Southern Ocean signature. *Journal of Geophysical Research Atmospheres* 105: 7187–7197. doi: 10.1029/1999JD901085

Dinniman M.S., Klinck J.M. and Hofmann E.E. 2012. Sensitivity of Circumpolar Deep Water transport and ice shelf basal melt along the West Antarctic Peninsula to changes in the winds. *Journal of Climate* 25: 4799–4816. doi: 10.1175/JCLI-D-11-00307.1

Dixon D., Mayewski P., Kaspari S., Sneed S. and Handley M. 2004. A 200 year sub-annual record of sulfate in West Antarctica, from 16 ice cores. *Annals of Glaciology* 39: 545–556. doi: 10.3189/172756404781814113

Earman S., Campbell A.R., Phillips F.M. and Newman B.D. 2006. Isotopic exchange between snow and atmospheric water vapor: estimation of the snowmelt component of groundwater recharge in the southwestern United States. *Journal of Geophysical Research* 111: D09302. doi: 10.1029/2005JD006470

Emanuelsson B.D., Bertler N.A.N., Neff P.D., Renwick J.A., Markle B.R., Baisden W.T. and Keller E.D. 2018. The role of Amundsen–Bellingshausen Sea anticyclonic circulation in forcing marine air intrusions into West Antarctica. *Climate Dynamics* 51: 3579–3596. doi: 10.1007/s00382-018-4097-3

Feldmann J. and Levermann A. 2015. Collapse of the West Antarctic Ice Sheet after local destabilization of the Amundsen Basin. *Proceedings of the National Academy of Sciences* 112: 14191–14196. doi: 10.1073/pnas.1512482112

Fogt R.L., Wovrosh A.J., Langen R.A. and Simmonds I. 2012. The characteristic variability and connection to the underlying synoptic activity of the Amundsen-Bellingshausen Seas Low. *Journal of Geophysical Research.* 117: D07111. doi: 10.1029/2011JD017337

Graham A.G.C., Wåhlin A., Hogan K.A., Nitsche F.O., Heywood K.J., Totten R.L., Smith J.A., Hillenbrand C-D., Simkins L.M., Anderson J.B., Wellner J.S. and Larter R.D. 2022. Rapid retreat of Thwaites Glacier in the pre-satellite era. *Nature Geoscience* 15: 706–713. doi: 10.1038/s41561-022-01019-9

Ham J., Hur S., Lee W., Han Y., Jung H. and Lee J. 2019. Isotopic variations of meltwater from ice by isotopic exchange between liquid water and ice. *Journal of Glaciology* 65: 1035–1043. doi: 10.1017/jog.2019.75

Helm V., Humbert A. and Miller H. 2014. Elevation and elevation change of Greenland and Antarctica derived from CryoSat-2. *The Cryosphere* 8: 1539–1559. doi: 10.5194/tc-8-1539-2014

Hong S.B., Hur S.D. and Kim S.M. 2012. Uncertainties of ionic species in snowpit samples determined with ion chromatography system. *Analytical Science and Technology of Korea* 25: 350–363. doi: 10.5806/AST.2012.25.6.350

Hosking J.S., Orr A., Marshall G.J., Turner J. and Phillips T. 2013. The influence of the Amundsen–Bellingshausen Seas low on the climate of West Antarctica and its representation in coupled climate model simulations. *Journal of Climate* 26: 6633–6648. doi: 10.1175/JCLI-D-12-00813.1

Hur S.D., Chung J., Nyamgerel Y. and Lee J. 2022. Seasonality of isotopic and chemical composition of snowpack in the vicinity of Jang Bogo Station, East Antarctica. *Polish Polar Research* 42: 221–236. doi: 10.24425/ppr.2021.137146

Jacob T., Wahr J., Pfeffer W. and Swenson S. 2012. Recent contributions of glaciers and ice caps to sea level rise. *Nature* 482: 514–518. doi: 10.1038/nature10847

Johnson J.S., Smith J.A., Schaefer J.M., Young N.E., Goehring B.M., Hillenbrand C.D., Lamp J.L., Finkel R.C. and Gohl K. 2017. The last glaciation of Bear Peninsula, central Amundsen Sea Embayment of Antarctica: Constraints on timing and duration revealed by in situ cosmogenic ^{14}C and ^{10}Be dating. *Quaternary Science Reviews* 178: 77–88. doi: 10.1016/j.quascirev.2017.11.003

Jonsell U., Hansson M.E., Mörth C-M. and Torssander P. 2005. Sulfur isotopic signals in two shallow ice cores from Dronning Maud Land, Antarctica. *Tellus B: Chemical and Physical Meteorology* 57: 341–350. doi: 10.3402/tellusb.v57i4.16558

Jouzel J. and Merlivat L. 1984. Deuterium and oxygen-18 in precipitation: Modeling of the isotope effects during snow formation. *Journal of Geophysics Research* 89: 11749–11757. doi: 10.1029/JD089iD07p11749

Jouzel J., Masson-Delmotte V., Cattani O., Dreyfus G., Falourd S., Hoffmann G., Minster B., Nouet J., Barnola J.M., Chappellaz J., Fischer H, Gallet J.C., Johnsen S., Leuenberger M., Loulergue L., Luethi D., Oerter H., Parrenin F., Raisbeck G., Raynaud D., Schilt A., Schwander J., Selmo E., Souchez R., Spahni R., Stauffer B., Steffensen J.P., Stenni B., Stocker T.F., Tison J. L., Werner M. and Wolff E.W. 2007. Orbital and millennial Antarctic climate variability over the past 800,000 years. *Science* 317: 793–796. doi: 10.1126/science.1141038

Kaspari S., Mayewski P., Dixon D., Spikes V., Sneed S., Handley M. and Hamilton G. 2004. Climate variability in West Antarctica derived from annual accumulation-rate records from ITASE firn/ice cores. *Annals of Glaciology* 39: 585–594. doi: 10.3189/172756404781814447

Klein F., Abram N.J., Curran M.A.J., Goosse H., Goursaud S., Masson-Delmotte V., Moy A., Neukom R., Orsi A., Sjolte J., Steiger N., Stenni B. and Werner M. 2019. Assessing the robustness of Antarctic temperature reconstructions over the past 2 millennia using pseudoproxy and data assimilation experiments. *Climate of the Past* 15: 661–684. doi: 10.5194/cp-15-661-2019

Kim B.H., Seo K.W., Eom J., Chen J. and Wilson C. 2020. Antarctic ice mass variations from 1979 to 2017 driven by anomalous precipitation accumulation. *Scientific Reports* 10: 20366. doi: 10.1038/s41598-020-77403-5

Kim S., Han C., Moon J., Han Y., Hur S.D. and Lee J. 2022. An optimal strategy for determining triple oxygen isotope ratios in natural water using a commercial cavity ring-down spectrometer. *Geoscience Journal* 26: 637–647. doi: 10.1016/j.gca.2004.02.010

Koffman B.G., Dowd E.G., Osterberg E.C., Ferris D.G., Hartman I.H., Wheatley S.D., Kurbatov A.V., Wong G.J., Markle B.R., Dunbar N.W., Kreutz K.J. and Yates M. 2017. Rapid transport of ash and sulfate from the 2011 Puyehue-Cordón Caulle (Chile) eruption to West Antarctica. *Journal of Geophysical Research Atmospheres* 122: 8908–8920. doi: 10.1002/2017JD026893

Kuramoto T., Goto-Azuma K., Hirabayashi M., Miyake T., Motoyama H., Dahl-Jensen D. and
    Steffensen J. 2011. Seasonal variations of snowchemistry at NEEM, Greenland. *Annals of
    Glaciology* 52: 193–200. doi: 10.3189/172756411797252365

Küttel M., Steig E.J., Ding Q., Monaghan A. J. and Battisti D.S. 2012. Seasonal climate
    information preserved in West Antarctic ice core water isotopes: relationships to temperature,
    large-scale circulation, and sea ice. *Climate Dynamics* 39: 1841–1857. doi: 10.1007/s00382-
    012-1460-7

Kwak H., Kang J-H., Hong S-B., Lee J., Chang C., Hur S.D. and Hong S. 2015. A study on high-
    resolution seasonal variations of major ionic species in recent snow near the Antarctic Jang
    Bogo Station. *Ocean & Polar Research.* 37: 127–140. doi: 10.4217/OPR.2015.37.2.127

Lee J., Feng X., Faiia A.M., Posmentier E.S., Kirchner J.W., Osterhuber R. and Taylor S. 2010.
    Isotopic evolution of a seasonal snowcover and its melt by isotopic exchange between liquid
    water and ice. *Chemical Geology* 270: 126–134. doi.org/10.1016/j.chemgeo.2009.11.011

Legrand M. and Mayewski P. 1997. Glaciochemistry of polar ice cores: A review. *Review of
    Geophysics* 35: 219–243. doi: 10.1029/96RG03527

Lilien D.A., Joughin I., Smith B. and Shean D.E. 2018. Changes in flow of Crosson and Dotson ice
    shelves, West Antarctica, in response to elevated melt. *The Cryosphere* 12: 1415–1431. doi:
    10.5194/tc-12-1415-2018

Liu H., Jezek K.C., Li B. and Zhao Z. 2015. Radarsat Antarctic Mapping Project Digital Elevation
    Model, Version 2. Boulder, Colorado USA. NASA National Snow and Ice Data Center
    Distributed Active Archive Center. doi: 10.5067/8JKNEW6BFRVD

Masson-Delmotte V., Hou S., Ekaykin A., Jouzel J., Aristarain A., Bernardo R.T., Bromwich D.,
    Attani O., Delmotte M., Falourd S., Frezzotti M., Gallée H., Genoni L., Isaksson E., Landais
    A., Helsen M.M., Hoffmann G., Lopez J., Morgan V., Motoyama H., Noone D., Oerter H.,
    Petit J.R., Royer A., Uemura R., Schmidt G.A., Schlosser E., Simões J.C., Steig E.J., Stenni
    B., Stievenard M., Van Den Broeke M.R., Van De Wal R.S.W., Van De Berg W.J., Vimeux F.
    and White J.W.C. 2008. A review of Antarctic surface snow isotopic composition:
    Observations, atmospheric circulation, and isotopic modeling. *Journal of Climate* 21:
    3359–3387. doi: 10.1175/2007JCLI2139.1

Matsuoka K., Hindmarsh R.C., Moholdt G., Bentley M.J., Pritchard H.D., Brown J., Conway H.,
    Drews R., Durand G., Goldberg D., Hattermann T., Kingslake J., Lenaerts J.T.M., Martín C.,
    Mulvaney R., Nicholls K.W., Pattyn F., Ross N., Scambos T. and Whitehouse P.L. 2015.
    Antarctic ice rises and rumples: Their properties and significance for icesheet dynamics and
    evolution. *Earth-Science Reviews* 150: 724–745. doi: 10.1016/j.earscirev.2015.09.004

Matsuoka K., Skoglund A., Roth G., de Pomereu J., Griffiths H., Headland R., Herried B.,
    Katsumata K., Le Brocq A., Licht K., Neff P.D., Scheinert M., Tamura T., Van de Putte A.,
    van den Broeke M., Von Deschwanden A., Deschamps-Berger C., Van Liefferinge B.,
    Tronstad S. and Melvær Y. 2021. Quantarctica, an integrated mapping environment for
    Antarctica, the southern ocean, and subantarctic islands. *Environmental Modelling &
    Software* 140: 105015. doi: 10.1016/j.envsoft.2021.105015

Medley B., Joughin I., Das S.B., Steig W.J., Conway H., Gogineni S., Criscitiello A.S., McConnell
    J.R., Smith B.E., van den Broeke M.R., Lenaerts A. S., Bromwich D.H. and Nicolas J.P. 2013.
    Airborne-radar and ice-core observations of annual snow accumulation over Thwaites
    Glacier, West Antarctica confirm the spatiotemporal variability of global and regional
    atmospheric models. *Geophysical Research Letters* 40: 3649–3654. doi: 10.1002/grl.50706

Mouginot J., Scheuchl B. and Rignot E. 2012. Mapping of ice motion in Antarctica using synthetic-
    aperture radar data. *Remote Sensing* 4: 2753–2767. doi: 10.3390/rs4092753

Mouginot J., Rignot E. and Scheuchl B. 2013. Sustained increase in ice discharge from the
    Amundsen Sea Embayment, West Antarctica, from 1973 to 2013. *Geophysical Research
    Letters* 41: 1576–1584. doi: 10.1002/2013GL059069

Mouginot J., Rignot E., Scheuchi B. and Millan R. 2017. Comprehensive annual ice sheet velocity mapping using Landsat-8, Sentinel-1, and RADARSAT-2 data. *Remote Sensing* 9: 364. doi: 10.3390/rs9040364

Mulvaney R., Rix, J., Polfrey S., Grieman M., Martin, C., Nehrbass-Ahles C., Rowell S., Tuckwell R. and Wolff E. 2021. Ice drilling on Skytrain Ice Rise and Sherman Island, Antarctica. *Annals of Glaciology* 62: 311–323. doi: 10.1017/aog.2021.7

Neff P. 2020. Amundsen Sea coastal ice rises: Future sites for marine-focused ice core records. *Oceanography* 33: 88–89. doi: 10.5670/oceanog.2020.215

Nyamgerel Y., Han Y., Kim S., Hong S., Lee J. and Hur S. 2000. Chronological characteristics for snow accumulation on Styx Glacier in northern Victoria Land, Antarctica. *Journal of Glaciology* 66: 916–926. doi: 10.1017/jog.2020.53

Parkinson C.L. and Cavalieri D.J. 2012. Antarctic sea ice variability and trends, 1979–2010. *The Cryosphere* 6: 871–880. doi: 10.5194/tc-6-871-2012

Pasteris D.R., Mcconnell J.R., Das S.B., Criscitiello A.S., Evans M.J., Maselli O.J., Sigl M. and Layman L. 2014. Seasonally resolved ice core records from West Antarctica indicate a sea ice source of sea-salt aerosol and a biomass burning source of ammonium. *Journal of Geophysical Research: Atmospheres* 119: 9168–9182. doi: 10.1002/2013JD020720

Pereira P.S., Flierdt T.V.D., Hemming S.R., Frederichs T., Hammond S.J., Brachfeld S., Doherty C., Kuhn G., Smith J.A., Klages J.P. and Hillenbrand C.-D. 2020. The geochemical and mineralogical fingerprint of West Antarctica's weak underbelly: Pine Island and Thwaites glaciers. *Chemical Geology* 550: 119649. doi: 10.1016/j.chemgeo.2020.119649

Petit J.R., Jouzel J., Raynaud D., Barkov N.I., Barnola J.-M., Basile I., Bender M., Chappellaz J., Davis M., Delaygue G., Delmotte M., Kotlyakov V.M., Legrand M., Lipenkov V.Y., Lorius C., Pépin L., Ritz C., Saltzman E. and Stievenard M. 1999. Climate and atmospheric history of the past 420,000 years from the Vostok ice core, Antarctica. *Nature* 399: 429–436. doi: 10.1038/20859

Pilson M.E.Q. 2013. *An Introduction to the Chemistry of the Sea.* (2nd edition). Cambridge University Press, New York.

Rankin A.M., Auld V. and Wolff E.W. 2000. Frost flowers as a source of fractionated sea salt aerosol in the polar regions. *Geophysical Research Letters* 27: 3469–3472. doi: 10.1029/2000GL011771

Raphael M.N., Marshall G.J., Turner J., Fogt R.L., Schneider D., Dixon D.A., Hosking J.S., Jones J.M. and Hobbs W.R. 2016. The Amundsen Sea low: Variability, change and impact on Antarctic climate. *Bulletin of the American Meteorological Society* 97: 111–121. doi: 10.1175/BAMS-D-14-00018.1

Rhodes R.H., Bertler N.A.N., Baker J.A., Steen-Larsen H.C., Sneed S.B., Morgenstern U. and Johnsen S.J. 2012. Little Ice Age climate and oceanic conditions of the Ross Sea, Antarctica from a coastal ice core record. *Climate of the Past* 8: 1223–1238. doi: 10.5194/cp-8-1223-2012

Rignot E., Mouginot J. and Scheuchl B. 2011. Ice flow of the Antarctic Ice Sheet. *Science* 333: 1427–1430. doi: 10.1126/science.1208336

Rignot E., Mouginot J. and B. Scheuchl. 2017. MEaSUREs InSAR-Based Antarctica Ice Velocity Map, Version 2 [Data Set]. Boulder, Colorado USA. NASA National Snow and Ice Data Center Distributed Active Archive Center. 10.5067/D7GK8F5J8M8R. Date Accessed 03-12-2023.

Scarchilli C., Frezzotti M. and Ruti P.M. 2011. Snow precipitation at four ice core sites in East Antarctica: Provenance, seasonality and blocking factors. *Climate Dynamics* 37: 2107–2125. doi: 10.1007/s00382-010-0946-4

Sinclair K.E., Bertler N.A.N. and Trompetter W.J. 2010. Synoptic controls on precipitation pathways and snow delivery to high-accumulation ice core sites in the Ross Sea region, Antarctica. *Journal of Geophysical Research* 115: D22112. doi: 10.1029/2010JD014383

Sinclair K.E., Bertler N.A.N., Bowen M. M. and Arrigo K.R. 2014. Twentieth century sea-ice trends in the Ross Sea from a high-resolution, coastal ice-core record. *Geophysical Research Letters* 41: 3510–3516. doi: 10.1002/2014GL059821

Stammerjohn S.E., Maksym T., Massom R. A., Lowry K.E., Arrigo K. R., Yuan X., Raphael M., Randall-Goodwin E.R., Sherrell R.M. and Yager P.L. 2015. Seasonal sea ice changes in the Amundsen Sea, Antarctica, over the period of 1979–2014. *Elementa: Science of the Anthropocene* 3: 000055. doi: 10.12952/journal.elementa.000055

Steig E.J. and Neff P.D. 2018. The prescience of paleoclimatology and the future of the Antarctic ice sheet. *Nature Communications* 9: 2730. doi: 10.1038/s41467-018-05001-1

Steig E.J., Ding Q., White J.W., Küttel M, Rupper S.B., Neumann T.A., Neff P.D., Gallant A.J., Mayewski P.A. and Taylor K.C. 2013. Recent climate and ice-sheet changes in West Antarctica compared with the past 2,000 years. *Nature Geoscience* 6: 372–375. doi: 10.1038/ngeo1778

Stenni B., Serra F., Frezzotti M., Maggi V., Traversi R., Becagli S. and Udisti R. 2000. Snow accumulation rates in northern Victoria Land, Antarctica, by firn-core analysis. *Journal of Glaciology* 46: 541–552. doi: 10.3189/172756500781832774

Stenni B., Curran M.A.J., Abram N.J., Orsi A., Goursaud S., Masson-Delmotte V., Neukom R., Goosse H., Divine D., Van Ommen T., Steig E.J., Dixon D.A., Thomas E.R., Bertler N.A.N., Isaksson E., Ekaykin A., Werner M. and Frezzotti M. 2017. Antarctic climate variability on regional and continental scales over the last 2000 years. *Climate of the Past* 13: 1609–1634. doi: 10.5194/cp-13-1609-2017

Sutterley T.C., Velicogna I., Rignot, E., Mouginot J., Flament T., van den Broeke M.R., van Wessem J.M. and Reijmer C.H. 2014. Mass loss of the Amundsen Sea Embayment of West Antarctica from four independent techniques. *Geophysical Research Letters* 41: 8421–8428. doi: 10.1002/2014GL061940

Swetha Chittella S.P., Deb P. and Van Wessem J.M. 2022. Relative contribution of atmospheric drivers to "extreme" snowfall over the Amundsen Sea Embayment. *Geophysical Research Letters* 49: e2022GL098661. doi: 10.1029/2022GL098661

Thoma M., Jenkins A., Holland D. and Jacobs S. 2008. Modelling Circumpolar Deep Water intrusions on the Amundsen Sea continental shelf, Antarctica. *Geophysical Research Letters* 35: L18602. doi: 10.1029/2008GL034939

Thomas E.R., Hosking J.S., Tuckwell R.R., Warren R.A. and Ludlow E.C. 2015. Twentieth century increase in snowfall in coastal West Antarctica. *Geophysical Research Letters* 42: 9387–9393. doi: 10.1002/2015GL065750

Thomas E.R., Van Wessem M.J., Roberts J., Isaksson E., Schlosser E., Fudge T.J., Vallelonga P., Medley B., Lenaerts J. and Bertler N. 2017. Regional Antarctic snow accumulation over the past 1000 years. *Climate of the Past* 13: 1491–1513. doi: 10.5194/cp-13-1491-2017

Tuohy A., Bertler N., Neff P., Edwards R., Emanuelsson D., Beers T. and Mayewski P. 2015. Transport and deposition of heavy metals in the Ross Sea Region, Antarctica. *Journal of Geophysical Research: Atmosphere* 120: 10996–11011. doi: 10.1002/2015JD023293

Turner J., Orr, A., Gudmundsson G.H., Jenkins A., Bingham R.G., Hillenbrand C.-D. and Bracegirdle T.J. 2017. Atmosphere-ocean-ice interactions in the Amundsen Sea Embayment, West Antarctica. *Review of Geophysics* 55: 235–276. doi: 10.1002/2016RG000532

Turner J., Holmes, C., Caton Harrison T., Phillips T., Jena, B., Reeves-Francois T., Fogt, R., Thomas E.R. and Bajish C.C. 2022. Record low Antarctic sea ice cover in February 2022. *Geophysical Research Letters* 49: e2022GL098904. doi: 10.1029/2022GL098904

Udisti R., Traversi R., Becagli G. and Piccardi G. 1998. Spatial distribution and seasonal pattern of biogenic sulphur compounds in snow from northern Victoria Land, Antarctica R. *Annals of Glaciology* 27: 535–542. doi: 10.3189/1998AoG27-1-535-542

Vega C.P., Schlosser E., Divine D.V., Kohler J., Martma T., Eichler A., Schwikowski M. and Isaksson E. 2016. Surface mass balance and water stable isotopes derived from firn cores on

three ice rises, Fimbul Ice Shelf, Antarctica. *The Cryosphere* 10: 2763–2777. doi: 10.5194/tc-10-2763-2016

Wang Y., Yuan X., Bi, H., Liang Y., Huang H., Zhang Z. and Liu Y. 2019. The contributions of winter cloud anomalies in 2011 to the summer sea-ice rebound in 2012 in the Antarctic. *Journal of Geophysical Research: Atmospheres* 124: 3435–3447. doi: 10.1029/2018JD029435

Winstrup M., Vallelonga P., Kjær H.A., Fudge T.J., Lee J.E., Riis M.H., Edwards R., Bertler N.A.N., Blunier T., Brook E.J., Buizert C., Ciobanu G., Conway H., Dahl-Jensen D., Ellis A., Emanuelsson B.D., Hindmarsh R.C.A., Keller E.D., Kurbatov A.V., Mayewski P.A., Neff, P.D., Pyne R.L., Simonsen M.F., Svensson A., Tuohy A., Waddington E.D. and Wheatley S. 2019. A 2700-year annual timescale and accumulation history for an ice core from Roosevelt Island, West Antarctica. *Climate of the Past* 15: 751–779. doi: 10.5194/cp-15-751-2019

Yang J.-W., Han Y., Orsi A. J., Kim S.-J., Han H., Ryu Y., Jang Y., Moon J., Choe T., Hur S.D. and Ahn J. 2018. Surface temperature in twentieth century at the Styx Glacier, northern Victoria Land, Antarctica, from borehole thermometry. *Geophysical Research Letters* 45: 9834–9842. doi: 10.1029/2018GL078770

Zwally H.J., Robbins J.W., Luthcke S.B., Loomis B.D. and Rémy F. 2021. Mass balance of the Antarctic ice sheet 1992–2016: reconciling results from GRACE gravimetry with ICESat, ERS1/2 and Envisat altimetry. *Journal of Glaciology* 67: 533–559. doi: 10.1017/jog.2021.8